

On the stability of nucleic acid feedback controllers

Nuno M. G. Paulino^{†1}, Mathias Foo², Jongmin Kim³ and Declan G. Bates^{†4}

Abstract—Recent work has shown how chemical reaction network theory can be used to design synthetic feedback controllers. These controllers can be implemented biologically using nucleic acid-based chemistry based on DNA strand displacement reactions. Here, we show that such implementations can introduce hidden nonlinear dynamics (even in the case of linear controllers), which must be taken into account when analyzing their stability properties in the presence of inevitable experimental uncertainty.

Index Terms—Synthetic biology, Linear systems, Nonlinear systems, Chemical reaction networks, Feedback control

I. INTRODUCTION

One of the key needs of synthetic biology is the development of feedback control theory that can be used to design synthetic controllers for biomolecular processes [1]. A promising direction for this work is to exploit chemical reaction network (CRN) theory, since CRNs act as a “bridge” between mathematical design using ordinary differential equations (ODEs) and biological implementations using nucleic acid-based chemistry based on DNA strand displacement (DSD) reactions [2]–[4]. The ODE to CRN to DNA design framework [5], [6] assigns a formal species in the CRN to sets of DNA species, allowing the construction of circuits in a specific biological context [7]–[9], and providing a high level of automation using available syntax and software tools [10]–[12].

In the context of feedback control, a key challenge is to program CRNs to perform the subtraction operation between non-negative quantities, since implementation of this operator using CRNs generally results in a one-sided subtraction (i.e. it can only compute a positive difference between two inputs) [13]–[15]. This can lead to poor control performance or even instability [16], [17]. The approach in [13] circumvents this problem by representing each signal as the difference of concentrations of two different dual species, $x^+, x^- \in \mathbb{R}_0^+$. Although this *dual rail representation* [18] doubles the number of reactions required, it does allow the approximation and translation of linear feedback systems [14], [16], [17] and frequency representations [19] into DSD reactions, and has

recently been extended to include more complicated mathematical operators [6], nonlinear controllers [15], [20], and oscillators [21].

Since the same signal has infinitely many dual representations, for the purposes of experimental implementation very fast bimolecular annihilation reactions are put in place to keep one of the components close to zero. As we shall show later, these introduce additional nonlinear dynamics which are not observed in the input/output behavior of the nominal circuit CRN, but become important in the presence of parametric uncertainty and experimental variability of biomolecular implementations. In this note, we formally analyze these nonlinear dynamics in their natural coordinates – species concentrations – and highlight their potential impact on the stability of nucleic acid controllers under experimental variability. An early version of this paper appeared in [22].

II. CRN REPRESENTATION OF A LINEAR FEEDBACK CONTROL CIRCUIT

A CRN is composed of a set of reactions of chemical species X_j , where the chemical reaction can be approximated by sets of ODEs using mass action kinetics [23], i.e.,

$$\alpha_1 X_1 + \alpha_2 X_2 \xrightarrow{\gamma} \beta_1 X_1 + \beta_2 X_2 \Rightarrow \dot{x}_j = (\beta_j - \alpha_j) \gamma \prod_{i=1}^N x_i^{\alpha_i} \quad (1)$$

with γ representing the conversion rate. The stoichiometric coefficients α_j and β_j indicate, respectively, the relative number of molecules consumed and produced during the reaction. The variations in concentration x_j of each species X_j depend on the product of the concentrations, the power of their stoichiometric coefficients and the rate parameters.

If the dynamics of (1) are expressed in their natural coordinates, we have that the state vector contains the non-negative concentrations $x_j \in \mathbb{R}_0^+$. For any non-negative initial condition and non-negative input, the states remain $x_j(t) \geq 0, \forall t$, making the system non-negative [24] and invariant in the octant \mathbb{R}_0^{+N} . In the context of feedback control, the use of chemical concentrations as state variables is not suitable due to the aforementioned problem of one-sided subtraction, i.e. we require real signals $p_j \in \mathbb{R}$ to implement the control error $p_1 = r - y$ in the linear negative feedback of Fig. 1.

The framework of [13], [19] solves this problem by using a CRN representation of the system where each signal $p_j \in \mathbb{R}$ is represented by a dual representation [18] with $p_j = x_j^+ - x_j^-$. This framework requires only three types of reactions: catalysis $r \rightarrow r + x$, degradation $x \rightarrow \emptyset$, and annihilation $x_j^+ + x_j^- \xrightarrow{\eta} \emptyset$. The symbol \emptyset represents an empty result where the product is inactive (either due to degradation

[†]N. M. G. Paulino and D. G. Bates are with the Warwick Integrative Synthetic Biology Centre (WISB), School of Engineering, University of Warwick, Coventry CV4 7AL, UK ¹N.Paulino@warwick.ac.uk, ⁴D.Bates@warwick.ac.uk

²M. Foo is with the School of Mechanical, Aerospace and Automotive Engineering, Coventry University, Coventry CV1 5FB, UK Mathias.Foo@coventry.ac.uk

³J. Kim is with the Department of Integrative Bioscience and Biotechnology (IBB), Pohang University of Science and Technology (POSTECH), Pohang, Gyeongbuk, 37673, South Korea jongmin.kim@postech.ac.kr

D.G.B. acknowledges funding from the University of Warwick, the EPSRC/BBSRC Centre for Doctoral Training in Synthetic Biology (grant EP/L016494/1) and the BBSRC/EPSC Warwick Integrative Synthetic Biology Centre (grant BB/M017982/1)

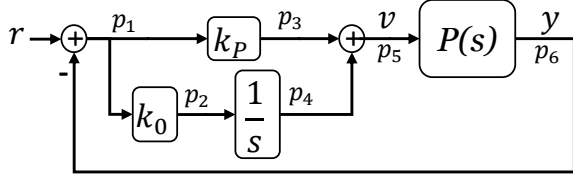
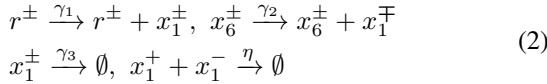
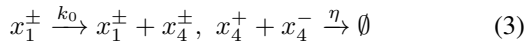


Fig. 1. Feedback interconnection for the linear dynamics where each signal p_j results from a linear operator.

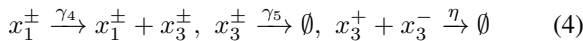
or sequestration) and no longer participates in the reactions. The dual representation admits infinite combinations, but since high species concentrations lead to problems with experimental implementation, such as unintended crosstalk among signal species, in practice annihilation reactions are used to minimize species concentrations by ensuring one of the concentrations is close to zero. This is achieved by setting the rate η to work on a much faster timescale than the dynamics of the system, to keep one of the components low even in the presence of transients. Using this framework, CRNs can be defined for each of the linear operations in the feedback system Fig. 1, where x_j^\pm represents simultaneously the two different species x_j^+ and x_j^- , and $x^\pm \xrightarrow{\gamma^\pm} y^\pm \Leftrightarrow x^+ \xrightarrow{\gamma^+} y^+, x^- \xrightarrow{\gamma^-} y^-$ [13], [15]. The corresponding reactions are as follows. For the subtraction $p_1 = r - p_6$ we have:



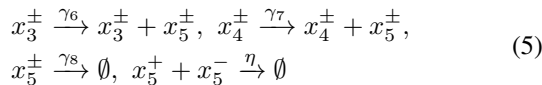
with $\gamma_1 = \gamma_2 = \gamma_3$. For the integral control $\dot{p}_4 = k_0 p_1$ we have



For the proportional gain $p_3 = k_P p_1$ we have



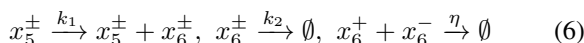
with $\gamma_4 = k_P \gamma_5$. The sum of signals $p_5 = p_3 + p_4$ is set with



and $\gamma_6 = \gamma_7 = \gamma_8$. We consider the plant $P(s)$ to be a first-order linear dynamical system with

$$Y(s) = \frac{k_1}{s + k_2} V(s)$$

This transfer function is approximated by the set of reactions



with $y = x_6^+ - x_6^-$ and $v = x_5^+ - x_5^-$, and parameterized by the rate constants k_1 and k_2 . Using mass action kinetics, the

corresponding ODEs for (2)-(6) are given by

$$\begin{aligned} \dot{x}_1^+ &= -\gamma_3 x_1^+ + \gamma_2 x_6^- + \gamma_1 r^+ - \eta x_1^+ x_1^- \\ \dot{x}_1^- &= -\gamma_3 x_1^- + \gamma_2 x_6^+ + \gamma_1 r^- - \eta x_1^+ x_1^- \\ \dot{x}_3^+ &= \gamma_4 x_1^+ - \gamma_5 x_3^+ - \eta x_3^+ x_3^- \\ \dot{x}_3^- &= \gamma_4 x_1^- - \gamma_5 x_3^- - \eta x_3^+ x_3^- \\ \dot{x}_4^+ &= k_0 x_1^+ - \eta x_4^+ x_4^- \\ \dot{x}_4^- &= k_0 x_1^- - \eta x_4^+ x_4^- \\ \dot{x}_5^+ &= \gamma_6 x_3^+ + \gamma_7 x_4^+ - \gamma_8 x_5^+ - \eta x_5^+ x_5^- \\ \dot{x}_5^- &= \gamma_6 x_3^- + \gamma_7 x_4^- - \gamma_8 x_5^- - \eta x_5^+ x_5^- \\ \dot{x}_6^+ &= k_1 x_5^+ - k_2 x_6^+ - \eta x_6^+ x_6^- \\ \dot{x}_6^- &= k_1 x_5^- - k_2 x_6^- - \eta x_6^+ x_6^- \end{aligned}$$

Reordering the ODEs with $\dot{p}_j = \dot{x}_j^+ - \dot{x}_j^-$ and $r = r^+ - r^-$ we arrive at the following standard representation of this set of CRN's as a linear state space system

$$\dot{\mathbf{p}} = A_p \mathbf{p} + B_p r \quad (7)$$

with $\mathbf{p} = [p_1 \ p_3 \ p_4 \ p_5 \ p_6]^T \in \mathbb{R}$, $r \in \mathbb{R}$ and

$$A_p = \begin{bmatrix} -\gamma_3 & 0 & 0 & 0 & -\gamma_2 \\ \gamma_4 & -\gamma_5 & 0 & 0 & 0 \\ k_0 & 0 & 0 & 0 & 0 \\ 0 & \gamma_6 & \gamma_7 & -\gamma_8 & 0 \\ 0 & 0 & 0 & k_1 & -k_2 \end{bmatrix}, \quad B_p = \begin{bmatrix} \gamma_1 \\ 0 \\ 0 \\ 0 \\ 0 \end{bmatrix}.$$

III. CLARIFYING THE NON-LINEAR DYNAMICS

It is important to note that the underlying dynamics for the natural coordinates x_j used to represent the linear feedback system shown in Fig. 1 using CRNs are *not*, in fact, linear, due to the presence of the annihilation reactions. To track the complete dynamics we need to capture in the ODEs the nonlinear terms from the bimolecular annihilation reactions, as follows. We keep the natural non-negative coordinates where the states are the species concentrations x_j^\pm , and the input vector contains both positive and negative components for the reference $\mathbf{r} = [r^+, r^-]^T$, $r^\pm \in \mathbb{R}_0^+$. The state is the vector of non-negative species concentrations

$$\begin{aligned} \mathbf{x} &= [x_1^+ \ x_2^+ \ \dots \ x_N^+ \mid x_1^- \ x_2^- \ \dots \ x_N^-]^T \in \mathbb{R}_0^{+2N} \\ &= [(\mathbf{x}^+)^T \mid (\mathbf{x}^-)^T]^T, \quad \mathbf{x}^\pm \in \mathbb{R}_0^{+N} \end{aligned} \quad (8)$$

The catalysis and degradation are unimolecular reactions depending linearly on the state, while the annihilation depends nonlinearly on the product of two states. This structures the system into a linear contribution, and a vector $\mathbf{g}\{\mathbf{x}\}$ with the nonlinear reactions fluxes

$$\mathbf{g}\{\mathbf{x}\} = \left[(\mathbf{x}^+ \circ \mathbf{x}^-)^T \quad (\mathbf{x}^+ \circ \mathbf{x}^-)^T \right]^T \quad (9)$$

where \circ represents the element-wise Hadamard product. Using these definitions we arrive at the nonlinear dynamics

$$\dot{\mathbf{x}} = A\mathbf{x} + B\mathbf{r} - \eta\mathbf{g}\{\mathbf{x}\} \quad (10)$$

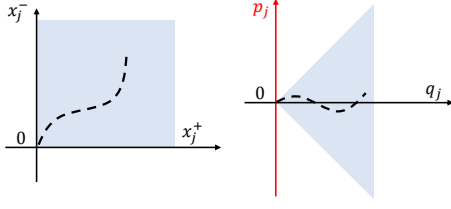


Fig. 2. Similarity transformation from the non-negative system with coordinates x_j^\pm on the left, to the new coordinates on the right with subtraction p_j and sum q_j of the pairs x_j^\pm . The invariant system of the trajectories changes from the positive octant on the left to the cone on the right, where trajectories projected on the ordinate are not restricted to be non-negative $p_j \in \mathbb{R}$, and $q_j \in \mathbb{R}_0^+$.

where the scalar η is the rate for the bimolecular annihilation reactions. We further decompose the dynamics according to the state partition in (8) so that

$$\begin{aligned}\dot{\mathbf{x}}^+ &= A_{11}^+ \mathbf{x}^+ + A_{12}^- \mathbf{x}^- + B_{11}^+ r^+ - \eta \mathbf{x}^+ \circ \mathbf{x}^- \\ \dot{\mathbf{x}}^- &= A_{12}^+ \mathbf{x}^+ + A_{11}^- \mathbf{x}^- + B_{11}^- r^- - \eta \mathbf{x}^+ \circ \mathbf{x}^- \end{aligned} \quad (11)$$

Because the catalysis and degradation reactions are duplicated for each pair of components x_i^\pm , matrices A and B are structured into

$$A = \begin{bmatrix} A_{11}^+ & A_{12}^- \\ A_{12}^+ & A_{11}^- \end{bmatrix}, \quad B = \begin{bmatrix} B_{11}^+ & 0 \\ 0 & B_{11}^- \end{bmatrix} \quad (12)$$

In the nominal case, where it is assumed that $\gamma_i = \gamma_j$, then $B_{11}^+ = B_{11}^-$ and $A_{ij}^+ = A_{ij}^-$. In reality, however, experimental variability will result in mismatches between reactions $\gamma_i \neq \gamma_j$ and also between the dual reactions with $\gamma_i^- \neq \gamma_i^+$, resulting in the matrices A_{ij}^+ and B_{11}^+ being populated with the reaction rates γ_i^+ , and their counterparts A_{ij}^- and B_{11}^- with γ_i^- . This model retains the nonlinearities required to track the impact of the fluxes due to the bimolecular reactions. Note that even in the presence of variability in the rates, the nonlinear terms are still canceled by $\dot{\mathbf{p}} = \dot{\mathbf{x}}^+ - \dot{\mathbf{x}}^-$, and hence the impact of these fluxes is not observed in the I/O linear dynamics given in (7).

A. Rotated nonlinear dynamics

The positivity of a system depends on the basis used for the state vector and usually results from using the natural coordinates of the system [24]. Here we expand on how the operation $\mathbf{p} = \mathbf{x}^+ - \mathbf{x}^-$ can be seen as a change of coordinates to remove the restrictive positivity of the states. Let us take the transformation

$$\begin{bmatrix} \mathbf{p} \\ \mathbf{q} \end{bmatrix} = \begin{bmatrix} -W_p \\ W_q \end{bmatrix} \mathbf{x} = \begin{bmatrix} I_N & -I_N \\ I_N & I_N \end{bmatrix} \mathbf{x} = [\Psi] \mathbf{x} \quad (13)$$

which rotates the state such that $p_j = x_j^+ - x_j^-$ and $q_j = x_j^+ + x_j^-$. This transformation is a global diffeomorphism [25], it is continuously differentiable, its Jacobian is non-singular $\forall x \in \mathbb{R}^{2N}$, and $\lim_{\|\mathbf{x}\| \rightarrow \infty} \|\Psi \mathbf{x}\| = \infty$. In this new set of coordinates, $p_j \in \mathbb{R}$, while q_j remains non-negative, (see Fig. 2). Given that $W_p \mathbf{g}\{\mathbf{x}\} = 0$, $W_q \mathbf{g}\{\mathbf{x}\} = 2(\mathbf{x}^+ \circ \mathbf{x}^-)$,

$[\Psi]^{-1} = \frac{1}{2} [\Psi]^T$, and the structure of A from (12), the dynamics in this rotated space can be written as

$$\begin{aligned} \begin{bmatrix} \dot{\mathbf{p}} \\ \dot{\mathbf{q}} \end{bmatrix} &= [\Psi] A [\Psi]^{-1} \begin{bmatrix} \mathbf{p} \\ \mathbf{q} \end{bmatrix} + [\Psi] B r - \eta \begin{bmatrix} 0 \\ 2(\mathbf{x}^+ \circ \mathbf{x}^-) \end{bmatrix} \\ &= R \begin{bmatrix} \mathbf{p} \\ \mathbf{q} \end{bmatrix} + \begin{bmatrix} W_p \\ W_q \end{bmatrix} B r - \frac{\eta}{2} \begin{bmatrix} 0 \\ \mathbf{q} \circ \mathbf{q} - \mathbf{p} \circ \mathbf{p} \end{bmatrix} \end{aligned} \quad (14)$$

where

$$\begin{aligned} R &= \begin{bmatrix} R_{11} & R_{12} \\ R_{21} & R_{22} \end{bmatrix} = \frac{1}{2} \begin{bmatrix} W_p A W_p^T & W_p A W_q^T \\ W_q A W_p^T & W_q A W_q^T \end{bmatrix} \\ &= \frac{1}{2} \begin{bmatrix} (A_{11}^+ + A_{11}^-) & (A_{11}^+ - A_{11}^-) \\ (A_{11}^+ - A_{11}^-) & (A_{11}^+ + A_{11}^-) \end{bmatrix} \\ &\quad + \frac{1}{2} \begin{bmatrix} -(A_{12}^+ + A_{12}^-) & -(A_{12}^+ - A_{12}^-) \\ (A_{12}^+ - A_{12}^-) & (A_{12}^+ + A_{12}^-) \end{bmatrix} \end{aligned} \quad (15)$$

B. Nominal case

Under the assumption of matching parameters $\gamma_i^+ = \gamma_i^-$, we have $A_{11}^+ = A_{11}^-$, $A_{12}^+ = A_{12}^-$, $B_{11}^+ = B_{11}^-$ and

$$R = \frac{1}{2} \begin{bmatrix} W_p A W_p^T & 0 \\ 0 & W_q A W_q^T \end{bmatrix} \quad (16)$$

This leads to a simplification in the *nominal dynamics* where the I/O linear system in (7) can be recovered through the similarity transformation $\mathbf{p} = W_p \mathbf{x}$

$$\dot{\mathbf{p}} = \frac{1}{2} W_p A W_p^T \mathbf{p} + W_p B r = (A_{11} - A_{12}) \mathbf{p} + B_{11} r \quad (17)$$

and linearity ensues from $W_p \mathbf{g}\{\mathbf{x}\} = 0$. Moreover, the *nominal rotated dynamics* have a cascaded structure

$$\begin{aligned} \dot{\mathbf{p}} &= R_{11} \mathbf{p} + W_p B r \\ \dot{\mathbf{q}} &= R_{22} \mathbf{p} + W_q B r - \frac{\eta}{2} (\mathbf{q} \circ \mathbf{q} - \mathbf{p} \circ \mathbf{p}) \end{aligned} \quad (18)$$

where the state \mathbf{q} does not affect the I/O linear state dynamics. The states p_i act as an input to \mathbf{q} , but \mathbf{p} evolves independently of \mathbf{q} . When the trajectories of x_i^\pm are collapsed into \mathbf{p} , the dynamics $\dot{\mathbf{q}}$ are not observable and the I/O dynamics (17) do not provide the complete information about the internal history of the species concentrations x_i^\pm .

IV. STABILITY ANALYSIS

The inevitable presence of experimental variability leads to mismatches between A_{ij}^\pm , and we lose the cascaded structure from (18) due to the cross-terms $W_p A W_q^T \neq 0$ and $W_q A W_p^T \neq 0$. Thus, the I/O linear system and the remaining dynamics become interconnected in a loop, and we need to analyze the stability of the complete nonlinear dynamics of (10). We investigate the stability of the nonlinear system using Lyapunov's indirect method, and the eigenvalues of the linearization at the equilibrium of the system. If for all eigenvalues λ_i of the linearization matrix results that $\Re\{\lambda_i\} < 0$ then the system is locally exponentially stable around the equilibrium [25]. To use this result we need to compute the equilibria of the system and the linearization about each equilibrium.

A. Computing the equilibria

The equilibria conditions for a null input $r^\pm = 0$ are given by the condition $A\mathbf{x}^0 - \eta\mathbf{x}^0 \circ \mathbf{x}^0 = 0$. Finding the solution besides the trivial $\mathbf{x} = 0$ is challenging due to the absence of a closed analytical solution. Moreover, if the equilibrium is unstable, then we cannot integrate the dynamics of (10) to find it.

However, for the dynamics of the rotated system, if $\mathbf{r} = 0$, half of the equilibrium conditions of (14) can be linearly expressed from the other half, with $\mathbf{p}^0 = -R_{11}^{-1}R_{12}\mathbf{q}^0$. We replace this solution in (14) and integrate instead the differential equations given by

$$\begin{aligned} \dot{\mathbf{q}} &= (R_{22} - R_{21}R_{11}^{-1}R_{12})\mathbf{q} \\ &+ \frac{\eta}{2} (R_{11}^{-1}R_{12}\mathbf{q}) \circ (R_{11}^{-1}R_{12}\mathbf{q}) - \frac{\eta}{2}\mathbf{q} \circ \mathbf{q} \end{aligned} \quad (19)$$

The equilibrium in the natural coordinates \mathbf{x} can then be recovered with

$$\mathbf{x}^0 = \frac{1}{2}[\Psi]^T \begin{bmatrix} \mathbf{p}^0 \\ \mathbf{q}^0 \end{bmatrix} = \frac{1}{2} \begin{bmatrix} \mathbf{q}^0 + \mathbf{p}^0 \\ \mathbf{q}^0 - \mathbf{p}^0 \end{bmatrix} \quad (20)$$

B. Perturbation model and linearization

The perturbed trajectories around the equilibrium are defined as $\mathbf{x}_e = \mathbf{x} - \mathbf{x}^0$ with perturbation input $\mathbf{r}_e = \mathbf{r} - \mathbf{r}^0$. Deriving the dynamics for $\dot{\mathbf{x}}_e = \dot{\mathbf{x}} - \dot{\mathbf{x}}^0 = \dot{\mathbf{x}}$ we have

$$\dot{\mathbf{x}}_e = (A + J\{\mathbf{x}^0\})\mathbf{x}_e + B\mathbf{r}_e - \eta\mathbf{g}\{\mathbf{x}_e\} \quad (21)$$

with

$$J\{\mathbf{x}^0\} = -\eta \begin{bmatrix} D\{\mathbf{x}^{0-}\} & D\{\mathbf{x}^{0+}\} \\ D\{\mathbf{x}^{0-}\} & D\{\mathbf{x}^{0+}\} \end{bmatrix}$$

and $D\{\mathbf{v}\}$ is a diagonal matrix with vector \mathbf{v} as diagonal. Linearizing the nonlinear model (10) around the equilibrium $\mathbf{x} = \mathbf{x}^0$ and $\mathbf{r}^0 = 0$ is equivalent to linearising the perturbation model around the origin $\mathbf{x}_e^0 = 0$, resulting in

$$\dot{\mathbf{s}} = A_s\mathbf{s} + B\mathbf{r}_e. \quad (22)$$

with $A_s = A + J\{\mathbf{x}^0\}$. The dependence on $J\{\mathbf{x}^0\}$ shows that for a non-Hurwitz matrix A , the linearization (22) can still be stable if a stable equilibrium $\mathbf{x}^0 > 0$ exists. Moreover, for the trivial equilibrium state $\mathbf{x}^0 = 0$ the linearized system is stable (and the nonlinear system is locally stable) if and only if A is Hurwitz.

V. ANALYSIS RESULTS

We now extend the example constructed in (7) by expressing the dynamics in the natural coordinates x_j^\pm under parametric variability, where the 22 rate parameters are allowed to vary. The nonlinear model (12) is parameterized according to

$$\begin{aligned} A_{11}^\pm &= \begin{bmatrix} -\gamma_3^\pm & 0 & 0 & 0 & 0 \\ \gamma_4^\pm & -\gamma_5^\pm & 0 & 0 & 0 \\ k_0^\pm & 0 & 0 & 0 & 0 \\ 0 & \gamma_6^\pm & \gamma_7^\pm & -\gamma_8^\pm & 0 \\ 0 & 0 & 0 & k_1^\pm & -k_2^\pm \end{bmatrix} \\ A_{12}^\pm &= \begin{bmatrix} \mathbf{0}_{1 \times 4} & \gamma_2^\pm \\ \mathbf{0}_{4 \times 4} & \mathbf{0}_{4 \times 1} \end{bmatrix}, \quad B_{11}^\pm = \begin{bmatrix} \gamma_1^\pm \\ \mathbf{0}_{4 \times 1} \end{bmatrix}, \end{aligned}$$

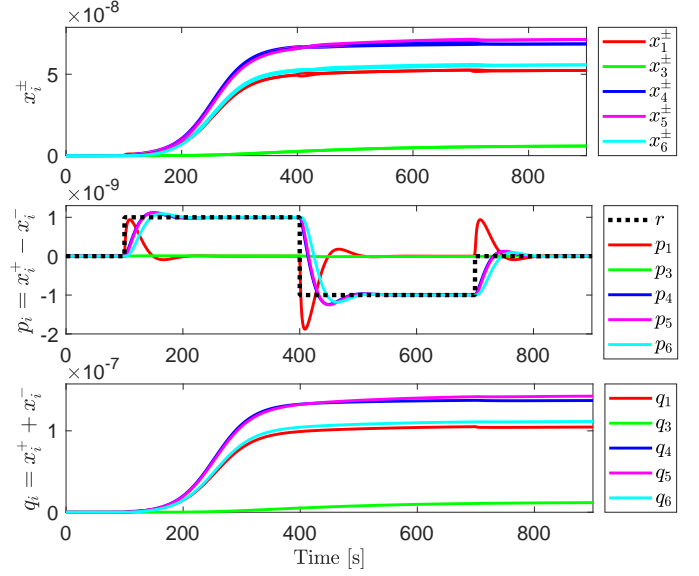


Fig. 3. Trajectories of the species concentrations x_j^\pm for the nominal parameterization and $x_j^\pm(0) = 10^{-12}$ M, and a sequence of reference steps. The rotated trajectories p_i and q_i are computed using (13). The I/O dynamics track the reference with a behavior approximate to a Proportional-Integral controller. The trajectories of \mathbf{q} depart from the origin and approach the stable equilibrium values $2\mathbf{x}^0$.

with the *nominal* values given in Table I. We also assume that the reference signal has only one of the concentrations r^+ or r^- at any given time, and consider the following example sequence of inputs

$$\begin{cases} 0 < t < 100s & r^+(t) = 0, r^-(t) = 0 \\ 100s \leq t < 400s & r^+(t) = 1 \text{ nM}, r^-(t) = 0 \\ 400s \leq t < 700s & r^+(t) = 0, r^-(t) = 1 \text{ nM} \\ t \geq 700s & r^+(t) = 0, r^-(t) = 0 \end{cases} \quad (23)$$

TABLE I
NOMINAL PARAMETERS FOR THE EXAMPLE [15], AND A
PARAMETERIZATION CASE WHICH RESULTS IN UNSTABLE DYNAMICS.

Parameter	Nominal	Destabilizing parameterization
k_1^\pm	0.1/s	0.132/s
k_2^\pm	0.1/s	0.068/s
$\gamma_i^\pm, i = 1, 2, 3$	0.4/s	$\gamma_1^+ = \gamma_2^\pm = \gamma_3^+ = 0.528/s,$ $\gamma_1^- = \gamma_3^- = 0.272/s$
$\gamma_i^\pm, i = 6, 7, 8$	0.8/s	$\gamma_6^\pm = \gamma_7^+ = 1.056/s, \gamma_7^- =$ $\gamma_8^\pm = 0.544/s$
$\gamma_i^\pm, i = 4, 5$	0.0004/s	$\gamma_4^+ = \gamma_5^- = 2.72 \times 10^{-4}/s,$ $\gamma_4^- = \gamma_5^+ = 5.28 \times 10^{-4}/s$
k_P^\pm	1	$\gamma_4^\pm/\gamma_5^\pm$
k_0^\pm	0.045/s	0.0594/s
η	$5 \times 10^5/\text{M/s}$	$5 \times 10^5/\text{M/s}$

In this case, A is not Hurwitz and $x_j^\pm = 0$ for $r^\pm = 0$ is an unstable equilibrium of the system. With $x_j^\pm(0) = 10^{-12}$ M, the nominal trajectories initially converge to the vicinity of the stable equilibrium, (see Fig. 3). Once the reference returns to $r^\pm = 0$ at $t = 700$ s the state converges to the stable equilibrium $\mathbf{x}^0 > 0$. The projected and orthogonal trajectories \mathbf{p} and \mathbf{q} are recovered with the map $[\Psi]$ from (13), where

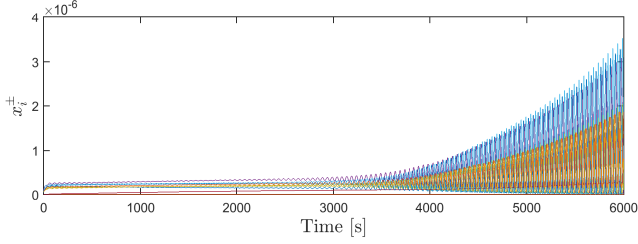


Fig. 4. Trajectories in natural coordinates x_i^\pm when parameterized with the mismatching rates from Table I, confirming the unstable behaviour of the system ($x_j^\pm(0) = 10^{-12} \text{ M}$, $\mathbf{r} = 0$).

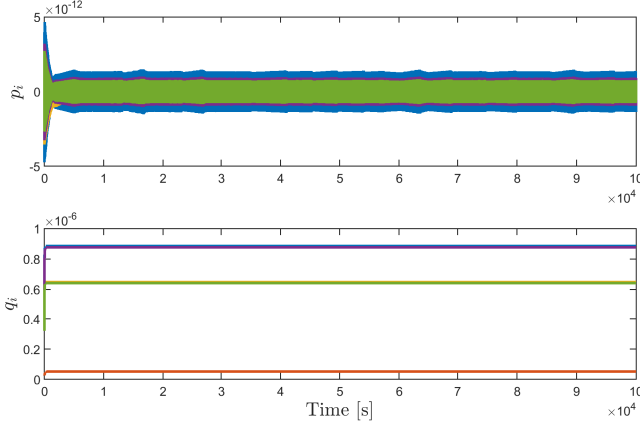


Fig. 5. Simulation of the rotated dynamics of $\tilde{\mathbf{p}}$ and $\tilde{\mathbf{q}}$ with decoupled matrix R where $R_{21} = R_{12} = 0$. If decoupled, both dynamics remain bounded for the same parameterization that destabilizes the interconnected nonlinear system.

the output p_6 tracks successfully the reference r , while $\mathbf{q} \geq 0$ reveals the underlying dynamics and the positive equilibrium concentrations.

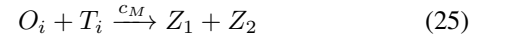
TABLE II
POLES OF THE LINEARIZED DYNAMICS FOR NOMINAL AND DESTABILIZING PARAMETERIZATION, AND POLES OF THE I/O LINEAR SYSTEM WITH DESTABILIZING PARAMETERIZATION

Linearization of nominal nonlinear dynamics $\lambda_i \{A_s\}$	$-0.8775, -0.7933, -0.4278, -0.4175, -0.2192, -0.0394 \pm i0.0522, -0.0350, -0.0061, -0.0004$
Linearization of unstable nonlinear dynamics $\lambda_i \{A_s\}$	$-0.9063, -0.5223, -0.4499 \pm i0.1387, -0.3943, +0.0032 \pm i0.1264, -0.1434, -0.0004, -0.0687$
I/O linear dynamics for the unstable nonlinear dynamics $\lambda_i \{R_{11}\}$	$-0.4571 \pm i0.0566, -0.0009 \pm i0.1255, -0.0005$

To account for realistic levels of experimental variability in the system we introduced an uncertainty of $\pm 33\%$ in the reaction rates, which includes the instance with mismatching rates in the last column of Table I. We perturbed the nonlinear dynamics for this case of interest around its equilibrium with $x_j(0) = 10^{-12} \text{ M}$, $\mathbf{r} = 0$ and we obtained a parameterization with an unstable response (see Fig. 4). Table II compares the poles of the linearizations for the nominal and the unstable parameterization, and shows that the linearization captures the instability in a pair of conjugated poles on the right-hand plane.

Crucially, however, the I/O linear system in the presence of variability is stable $\forall_i \Re(\lambda_i \{R_{11}\}) < 0$, even when the nonlinear system is not: $\exists_i \Re(\lambda_i \{A_s\}) > 0$ (in Table II). This was confirmed in Fig. 5 by integrating the rotated dynamics with a decoupled matrix R where we force $R_{21} = R_{12} = 0$. The perturbed dynamics remains stable and both $\tilde{\mathbf{p}}$ and $\tilde{\mathbf{q}}$ have bounded trajectories. This shows that the source of the instability of the complete nonlinear system is neither $\tilde{\mathbf{p}}$ nor $\tilde{\mathbf{q}}$ - it is only when the cross terms $W_p A W_q^T$ and $W_q A W_p^T$ are present that the system become unstable. We conclude that stability must be analyzed for the complete nonlinear dynamics (or its linearization) and that any analysis focusing solely on the I/O linear system can be misleading.

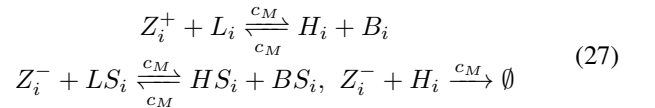
To verify whether our conclusions hold beyond the conceptual framework of CRN's, we tested our analysis on a network based explicitly on DNA chemistry [2], [3], [26]. Here, each of the catalysis, annihilation and degradation reactions in the CRN's were replaced by bimolecular DSD reactions [3], [13]. A catalysis reaction $Z_1 \xrightarrow{c_i} Z_1 + Z_2$ can be mapped into two unidirectional DSD reactions



with single strand DNA (ssDNA) species Z_1 , Z_2 , O_i and double strand DNA (dsDNA) species G_i and T_i . The intermediate species O_i serve as a map of identifiers between the reactant and the two products. The *gate* G_i and *translater* T_i species serve as translators of O_i decoupling completely the identifying sequences between different Z_i (further details in [3]). The unimolecular CRN reaction results into two bimolecular DSD reactions, and both produce *waste* in the form of inactivated dsDNA molecules which cannot participate in any reaction. As a consequence, the gate G_i and translater T_i are consumed irreversibly as *fuel*, and the reactions stop if these are not replenished. The degradation reactions $Z_i \xrightarrow{c_i} \emptyset$ are implemented with (24) where the gate species sequesters Z_i to produce an inactive dsDNA



Finally, the bimolecular annihilation reaction $Z_i^+ + Z_i^- \xrightarrow{c_M} \emptyset$ is translated into the set of DSD reactions



The *backward* strand B_i minimizes the use of Z_i^+ when Z_i^- is absent. The reversibility of the first reaction keeps H_i and Z_i^+ at equilibrium, allowing the conversion of unused H_i back to Z_i^+ . When both Z_i^\pm are present, H_i is irreversibly consumed, affecting the equilibrium and causing Z_i^+ to be used.

The associated ODEs are modeled using mass action kinetics and simulated using MATLAB (see Appendix). The model was parameterized with the unstable parameterization of Table I, with the rate constants scaled to implementable values of DSD reaction rates (see Appendix and [3] for rescaling details and procedure). The instability is also manifested in this DSD implementation (see Fig. 6), showing the practical relevance of the previous stability analysis.

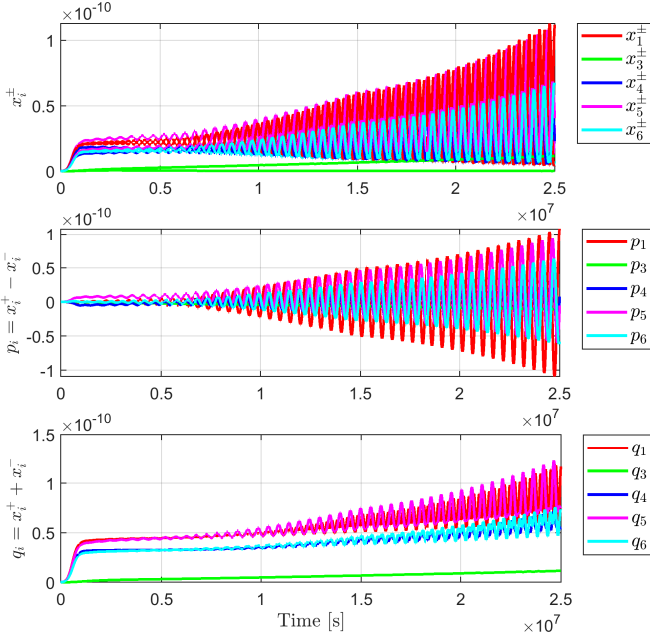


Fig. 6. Trajectories of the DSD reactions for the case of unstable CRNs, without input ($r(t) = 0$) and initial concentrations $x_i^\pm(0) = 10^{-13}$ M, $G_i^\pm(0) = T_i^\pm(0) = L_i^\pm(0) = B_i^\pm(0) = LS_i^\pm(0) = BS_i^\pm(0) = 10^{-5}$ M. The state starts by converging to the equilibrium, followed by the unstable behavior predicted by the nonlinear model of the CRNs. The DSD reaction rates are scaled with 10^{-3} , resulting in a system 10^3 times slower, and a signal reduction by a factor of 10^{-3} (see Appendix and [3] for details).

VI. CONCLUSIONS

Several recent works have applied the dual rail representation of CRN's to obtain linear I/O biochemical models of synthetic control systems, but have not explicitly considered the potential impact of the underlying nonlinear annihilation reactions in their analysis. We decomposed the dynamics of the CRN's and highlighted the effect of these non-observable and nonlinear dynamics. Specifically, we show that the stability of these I/O models does not imply the stability of the underlying chemical network. Under experimental variability, stability can be affected by the looped interconnection between the nonlinear dynamics arising from biological implementation and the linear I/O linear dynamics resulting from controller designs. We presented an example of this phenomenon, where the I/O linear system does not capture the instability of the full nonlinear system, and verified this result via simulation of the full DSD network. Our results confirm that the stability of nucleic acid-based controllers must be analyzed using the linearization of the complete nonlinear system, and provide a rigorous theoretical approach for conducting such an analysis.

REFERENCES

- [1] D. Del Vecchio, A. J. Dy, and Y. Qian, "Control theory meets synthetic biology," *Journal of Royal Society Interface*, vol. 13, no. 120, 2016.
- [2] Y.-J. Chen, N. Dalchau, N. Srinivas, A. Phillips, L. Cardelli, D. Soloveichik, and G. Seelig, "Programmable chemical controllers made from DNA," *Nature Nanotechnology*, vol. 8, no. 10, pp. 755–762, 2013.
- [3] D. Soloveichik, G. Seelig, and E. Winfree, "DNA as a universal substrate for chemical kinetics," *Proceedings of National Academy of Sciences*, vol. 107, no. 12, pp. 5393–5398, 2010.

- [4] C. Thachuk, E. Winfree, and D. Soloveichik, "Leakless DNA strand displacement systems," in *Lecture Notes in Computer Science*. Springer, Cham, 2015, vol. 9211, pp. 133–153.
- [5] N. Srinivas, J. Parkin, G. Seelig, E. Winfree, and D. Soloveichik, "Enzyme-free nucleic acid dynamical systems," *Science*, vol. 358, no. 6369, 2017.
- [6] M. Foo, R. Sawlekar, J. Kim, D. G. Bates, G. B. Stan, and V. Kulkarni, "Biomolecular implementation of nonlinear system theoretic operators," in *Proc. European Control Conf.*, Aalborg, Denmark, 2016, pp. 1824–1831.
- [7] A. K. George and H. Singh, "DNA implementation of fuzzy inference engine: towards DNA decision-making systems," *IEEE Transactions on NanoBioscience*, vol. 16, no. 8, pp. 773–782, dec 2017.
- [8] T. Song, S. Garg, R. Mokhtar, H. Bui, and J. Reif, "Design and analysis of compact DNA strand displacement circuits for analog computation using autocatalytic amplifiers," *ACS Synthetic Biology*, vol. 7, no. 1, pp. 46–53, jan 2018.
- [9] C. Zou, X. Wei, Q. Zhang, C. Liu, C. Zhou, and Y. Liu, "Four-analog computation based on DNA strand displacement," *ACS Omega*, vol. 2, no. 8, pp. 4143–4160, 2017.
- [10] A. Phillips and L. Cardelli, "A programming language for composable DNA circuits," *Journal Royal Society Interface*, vol. 6, no. Suppl_4, pp. S419–S436, 2009.
- [11] B. Yordanov, N. Dalchau, P. K. Grant, M. Pedersen, S. Emmott, J. Haseloff, and A. Phillips, "A computational method for automated characterization of genetic components," *ACS Synthetic Biology*, vol. 3, no. 8, pp. 578–588, 2014.
- [12] M. R. Lakin, R. L. Petersen, and A. P. Disclaimer, *Visual DSD user manual v0.14 beta*, 2017.
- [13] K. Oishi and E. Klavins, "Biomolecular implementation of linear I/O systems," *IET Systems Biology*, vol. 5, no. 4, pp. 252–260, 2011.
- [14] B. Yordanov, J. Kim, R. L. Petersen, A. Shudy, V. V. Kulkarni, and A. Phillips, "Computational design of nucleic acid feedback control circuits," *ACS Synthetic Biology*, vol. 3, no. 8, pp. 600–616, aug 2014.
- [15] M. Foo, R. Sawlekar, and D. G. Bates, "Exploiting the dynamic properties of covalent modification cycle for the design of synthetic analog biomolecular circuitry," *Journal of Biological Engineering*, vol. 10, no. 1, p. 15, 2016.
- [16] M. Foo, J. Kim, J. Kim, and D. G. Bates, "Proportional-integral degradation control allows accurate tracking of biomolecular concentrations with fewer chemical reactions," *IEEE Life Sciences Letters*, vol. 2, no. 4, pp. 55–58, 2016.
- [17] M. Foo, J. Kim, R. Sawlekar, and D. G. Bates, "Design of an embedded inverse-feedforward biomolecular tracking controller for enzymatic reaction processes," *Computers & Chemical Engineering*, vol. 99, pp. 145 – 157, 2017.
- [18] H.-L. Chen, D. Doty, and D. Soloveichik, "Rate-independent computation in continuous chemical reaction networks," in *Proc. 5th Conf. on Innovations in Theoretical Computer Science*, 2014, pp. 313–326.
- [19] T. Y. Chiu, H. J. K. Chiang, R. Y. Huang, J. H. R. Jiang, and F. Fages, "Synthesizing configurable biochemical implementation of linear systems from their transfer function specifications," *PLoS ONE*, vol. 10, no. 9, p. e0137442, 2015.
- [20] R. Sawlekar, F. Montefusco, V. V. Kulkarni, and D. G. Bates, "Implementing nonlinear feedback controllers using DNA strand displacement reactions," *IEEE Transactions on NanoBioscience*, vol. 15, no. 5, pp. 443–454, 2016.
- [21] C. Zou, X. Wei, Q. Zhang, and Y. Liu, "Synchronization of chemical reaction networks based on DNA strand displacement circuits," *IEEE Access*, vol. 6, pp. 20 584–20 595, 2018.
- [22] N. M. G. Paulino, M. Foo, J. Kim, and D. G. Bates, "Uncertainty modelling and stability robustness analysis of nucleic acid-based feedback control systems," in *Proc. 57th IEEE Conf. on Decision and Control*, Florida, 2018.
- [23] P. Tóth and J. Érdi, *Mathematical models of chemical reactions: Theory and Applications of Deterministic and Stochastic Models*. Manchester University Press, 1989.
- [24] L. Farina and S. Rinaldi, *Positive linear systems: theory and applications*. Wiley, 2000.
- [25] H. Khalil, *Nonlinear control, Global Edition*. Essex, England: Pearson Education Limited, 2015.
- [26] N. Srinivas, T. E. Ouldridge, P. Šulc, J. M. Schaeffer, B. Yurke, A. A. Louis, J. P. K. Doye, and E. Winfree, "On the biophysics and kinetics of toehold-mediated DNA strand displacement," *Nucleic Acids Research*, vol. 41, no. 22, pp. 10 641–10 658, 2013.

APPENDIX

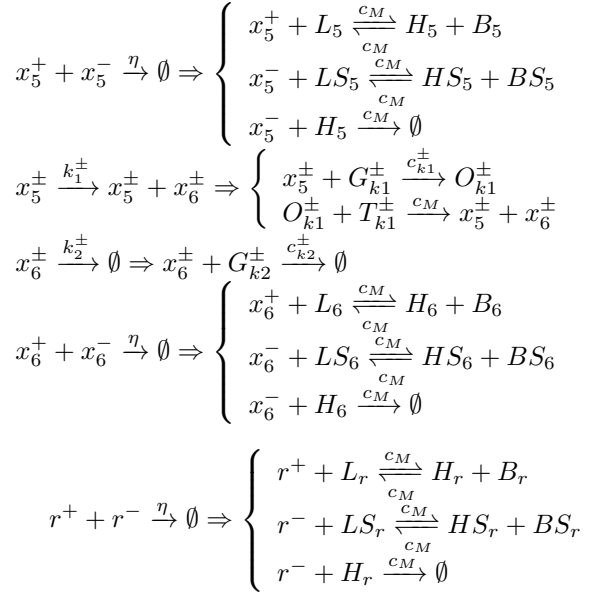
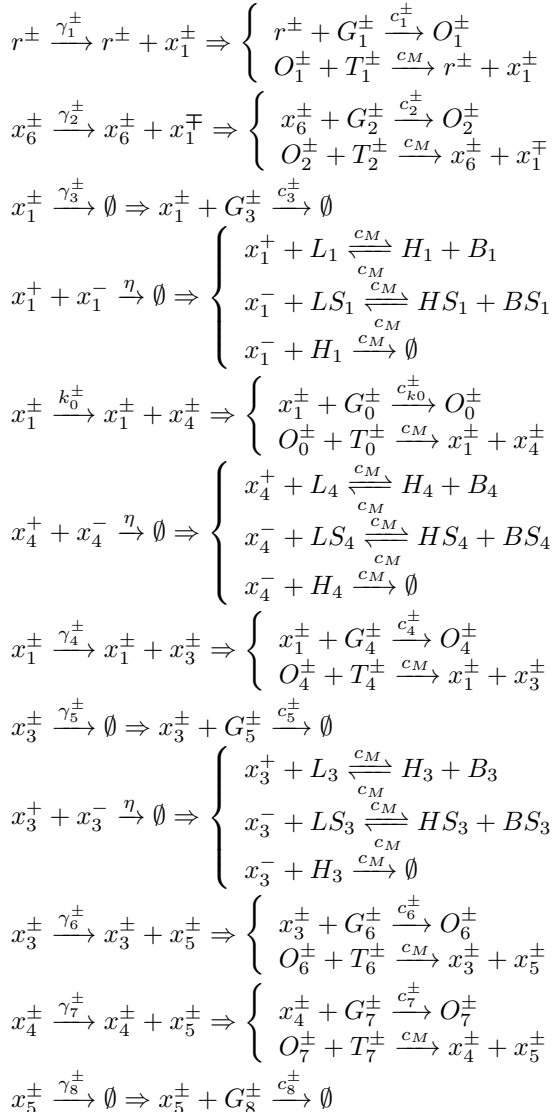
A. Reactions for DNA implementation

The translation of the CRN system to DSD reactions follows the construction proposed in [3] and adopted in [13].

The rates from the original CRN can be too high for implementation, since the DSD reactions are experimentally limited by maximum rates. This is addressed by the rescaling procedure proposed in [3] where, for a scaling factor δ , the species concentrations and all the unimolecular rate constants are reduced by a factor of δ , and the time scale increases by a factor of δ . The solutions to the ODEs are equivalent but in a different timescale [3]. In our case, we apply a factor of $\delta = 10^3$ to scale the down the rates by $1/\delta$.

The correspondence between the reaction rates in the CRN and the DSD implementation is: $c_M = 2\eta$, $c_{ki}^\pm = 2k_i^\pm / (\delta C_{max})$, $i \in \{0, 1, 2\}$, and $c_i^\pm = 2\gamma_i^\pm / (\delta C_{max})$, $i \in \{1, \dots, 8\}$. C_{max} is the initial concentration of the auxiliary species is $G_i^\pm(0) = T_i^\pm(0) = L_i^\pm(0) = B_i^\pm(0) = LS_i^\pm(0) = BS_i^\pm(0) = C_{max} = 10^{-5} \text{ M}$.

We list here the DSD reactions for the reaction networks defined in (2), (3), (4), (5) and (6).



B. ODEs for DNA implementation

Using mass action kinetics [23], the approximated ODEs are as follows:

$$\begin{aligned}
 \dot{r}^+ &= -c_1^+ G_1^+ r^+ + c_M O_1^+ T_1^+ - c_M r^+ L_r + c_M H_r B_r \\
 \dot{r}^- &= -c_1^- G_1^- r^- + c_M O_1^- T_1^- - c_M r^- H_r \\
 &\quad - c_M r^- L_r + c_M H_r B_r \\
 \dot{x}_1^+ &= c_M O_1^+ T_1^+ + c_M O_2^- T_2^- - c_4^+ x_1^+ G_4^+ + c_M O_4^+ T_4^+ \\
 &\quad - c_{k0}^+ x_1^+ G_0^+ + c_M O_0^+ T_0^+ - c_3^+ x_1^+ G_3^+ \\
 &\quad - c_M x_1^+ L_1 + c_M H_1 B_1 \\
 \dot{x}_1^- &= c_M O_1^- T_1^- + c_M O_2^+ T_2^+ - c_4^- x_1^- G_4^- + c_M O_4^- T_4^- \\
 &\quad - c_{k0}^- x_1^- G_0^- + c_M O_0^- T_0^- - c_3^- x_1^- G_3^- \\
 &\quad - c_M x_1^- L_1 + c_M H_1 B_1 \\
 \dot{x}_3^+ &= c_M O_4^+ T_4^+ - c_5^+ x_3^+ G_5^+ - c_M x_3^+ L_3 + c_M H_3 B_3 \\
 \dot{x}_3^- &= c_M O_4^- T_4^- - c_5^- x_3^- G_5^- \\
 &\quad - c_M x_3^- L_3 + c_M H_3 B_3 - c_M x_3^- H_3 \\
 \dot{x}_4^+ &= c_M O_0^+ T_0^+ - c_7^+ x_4^+ G_7^+ + c_M O_7^+ T_7^+ \\
 &\quad - c_M x_4^+ L_4 + c_M H_4 B_4 \\
 \dot{x}_4^- &= + c_M O_0^- T_0^- - c_7^- x_4^- G_7^- + c_M O_7^- T_7^- \\
 &\quad - c_M x_4^- L_4 + c_M H_4 B_4 - c_M x_4^- H_4 \\
 \dot{x}_5^+ &= -c_{k1}^+ G_{k1}^+ x_5^+ + c_M O_{k1}^+ T_{k1}^+ + c_M O_6^+ T_6^+ \\
 &\quad + c_M O_7^+ T_7^+ - c_8^+ x_5^+ G_8^+ - c_M L_5^+ x_5^+ + c_M H_5 B_5 \\
 \dot{x}_5^- &= -c_{k1}^- G_{k1}^- x_5^- + c_M O_{k1}^- T_{k1}^- + c_M O_6^- T_6^- \\
 &\quad + c_M O_7^- T_7^- - c_8^- x_5^- G_8^- \\
 &\quad - c_M L_5^- x_5^- + c_M H_5 B_5 - c_M x_5^- H_5 \\
 \dot{x}_6^+ &= + c_M O_{k1}^+ T_{k1}^+ - c_{k2}^+ x_6^+ G_{k2}^+ \\
 &\quad - c_M L_6^+ x_6^+ + c_M H_6 B_6 \\
 \dot{x}_6^- &= + c_M O_{k1}^- T_{k1}^- - c_{k2}^- x_6^- G_{k2}^- \\
 &\quad - c_M L_6^- x_6^- + c_M H_6 B_6 - c_M x_6^- H_6
 \end{aligned}$$

The concentrations of the auxiliary chemical species are governed by:

$$\begin{aligned}
\bullet r^\pm \xrightarrow{\gamma_1^\pm} r^\pm + x_1^\pm &\Rightarrow \begin{cases} \dot{G}_1^\pm = -c_1^\pm G_1^\pm r^\pm \\ \dot{O}_1^\pm = c_1^\pm G_1^\pm r^\pm - c_M O_1^\pm T_1^\pm \\ \dot{T}_1^\pm = -c_M O_1^\pm T_1^\pm \end{cases} \\
\bullet x_6^\pm \xrightarrow{\gamma_2^\pm} x_6^\pm + x_1^\mp &\Rightarrow \begin{cases} \dot{G}_2^\pm = -c_2^\pm G_2^\pm x_6^\pm \\ \dot{O}_2^\pm = c_2^\pm G_2^\pm x_6^\pm - c_M O_2^\pm T_2^\pm \\ \dot{T}_2^\pm = -c_M O_2^\pm T_2^\pm \end{cases}
\end{aligned}$$

$$\begin{aligned}
\bullet x_1^\pm \xrightarrow{\gamma_3^\pm} \emptyset &\Rightarrow \dot{G}_3^\pm = -c_3^\pm x_1^\pm G_3^\pm \\
\bullet x_1^+ + x_1^- \xrightarrow{\eta} \emptyset &\Rightarrow
\end{aligned}$$

$$\begin{cases} \dot{L}_1 = -c_M x_1^+ L_1 + c_M H_1 B_1 \\ \dot{H}_1 = +c_M x_1^+ L_1 - c_M H_1 B_1 - c_M x_1^- H_1 \\ \dot{B}_1 = +c_M x_1^+ L_1 - c_M H_1 B_1 \\ \dot{L}S_1 = -c_M x_1^- L S_1 + c_M H S_1 B S_1 \\ \dot{H}S_1 = +c_M x_1^- L S_1 - c_M H S_1 B S_1 \\ \dot{B}S_1 = +c_M x_1^- L S_1 - c_M H S_1 B S_1 \end{cases}$$

$$\bullet x_1^\pm \xrightarrow{k_0^\pm} x_1^\pm + x_4^\pm \Rightarrow \begin{cases} \dot{G}_0^\pm = -c_{k_0}^\pm x_1^\pm G_0^\pm \\ \dot{O}_0^\pm = c_{k_0}^\pm x_1^\pm G_0^\pm - c_M O_0^\pm T_0^\pm \\ \dot{T}_0^\pm = -c_M O_0^\pm T_0^\pm \end{cases}$$

$$\bullet x_4^+ + x_4^- \xrightarrow{\eta} \emptyset \Rightarrow$$

$$\begin{cases} \dot{L}_4 = -c_M x_4^+ L_4 + c_M H_4 B_4 \\ \dot{H}_4 = +c_M x_4^+ L_4 - c_M H_4 B_4 - c_M x_4^- H_4 \\ \dot{B}_4 = +c_M x_4^+ L_4 - c_M H_4 B_4 \\ \dot{L}S_4 = -c_M x_4^- L S_4 + c_M H S_4 B S_4 \\ \dot{H}S_4 = +c_M x_4^- L S_4 - c_M H S_4 B S_4 \\ \dot{B}S_4 = +c_M x_4^- L S_4 - c_M H S_4 B S_4 \end{cases}$$

$$\bullet x_1^\pm \xrightarrow{\gamma_4^\pm} x_1^\pm + x_3^\pm \Rightarrow \begin{cases} \dot{G}_4^\pm = -c_4^\pm x_1^\pm G_4^\pm \\ \dot{O}_4^\pm = c_4^\pm x_1^\pm G_4^\pm - c_M O_4^\pm T_4^\pm \\ \dot{T}_4^\pm = -c_M O_4^\pm T_4^\pm \end{cases}$$

$$\bullet x_3^\pm \xrightarrow{\gamma_5^\pm} \emptyset \Rightarrow \dot{G}_5^\pm = -c_5^\pm x_3^\pm G_5^\pm$$

$$\bullet x_3^+ + x_3^- \xrightarrow{\eta} \emptyset \Rightarrow$$

$$\begin{cases} \dot{L}_3 = -c_M x_3^+ L_3 + c_M H_3 B_3 \\ \dot{H}_3 = +c_M x_3^+ L_3 - c_M H_3 B_3 - c_M x_3^- H_3 \\ \dot{B}_3 = +c_M x_3^+ L_3 - c_M H_3 B_3 \\ \dot{L}S_3 = -c_M x_3^- L S_3 + c_M H S_3 B S_3 \\ \dot{H}S_3 = +c_M x_3^- L S_3 - c_M H S_3 B S_3 \\ \dot{B}S_3 = +c_M x_3^- L S_3 - c_M H S_3 B S_3 \end{cases}$$

$$\bullet x_3^\pm \xrightarrow{\gamma_6^\pm} x_3^\pm + x_5^\pm \Rightarrow \begin{cases} \dot{G}_6^\pm = -c_6^\pm x_3^\pm G_6^\pm \\ \dot{O}_6^\pm = c_6^\pm x_3^\pm G_6^\pm - c_M O_6^\pm T_6^\pm \\ \dot{T}_6^\pm = -c_M O_6^\pm T_6^\pm \end{cases}$$

$$\bullet x_4^\pm \xrightarrow{\gamma_7^\pm} x_4^\pm + x_5^\pm \Rightarrow \begin{cases} \dot{G}_7^\pm = -c_7^\pm x_4^\pm G_7^\pm \\ \dot{O}_7^\pm = c_7^\pm x_4^\pm G_7^\pm - c_M O_7^\pm T_7^\pm \\ \dot{T}_7^\pm = -c_M O_7^\pm T_7^\pm \end{cases}$$

$$\bullet x_5^\pm \xrightarrow{\gamma_8^\pm} \emptyset \Rightarrow \dot{G}_8^\pm = -c_8^\pm x_5^\pm G_8^\pm$$

$$\bullet x_5^+ + x_5^- \xrightarrow{\eta} \emptyset \Rightarrow$$

$$\begin{cases} \dot{L}_5 = -c_M L_5 x_5^+ + c_M H_5 B_5 \\ \dot{H}_5 = +c_M L_5 x_5^+ - c_M H_5 B_5 - c_M x_5^- H_5 \\ \dot{B}_5 = +c_M L_5 x_5^+ - c_M H_5 B_5 \\ \dot{L}S_5 = -c_M L S_5 x_5^- + c_M H S_5 B S_5 \\ \dot{H}S_5 = +c_M L S_5 x_5^- - c_M H S_5 B S_5 \\ \dot{B}S_5 = +c_M L S_5 x_5^- - c_M H S_5 B S_5 \end{cases}$$

$$\bullet x_5^\pm \xrightarrow{k_1^\pm} x_5^\pm + x_6^\pm \Rightarrow \begin{cases} \dot{G}_{k1}^\pm = -c_{k1}^\pm x_5^\pm G_{k1}^\pm \\ \dot{O}_{k1}^\pm = c_{k1}^\pm x_5^\pm G_{k1}^\pm - c_M O_{k1}^\pm T_{k1}^\pm \\ \dot{T}_{k1}^\pm = -c_M O_{k1}^\pm T_{k1}^\pm \end{cases}$$

$$\bullet x_6^\pm \xrightarrow{k_2^\pm} \emptyset \Rightarrow \dot{G}_{k2}^\pm = -c_{k2}^\pm x_6^\pm G_{k2}^\pm$$

$$\bullet x_6^+ + x_6^- \xrightarrow{\eta} \emptyset \Rightarrow$$

$$\begin{cases} \dot{L}_6 = -c_M L_6 x_6^+ + c_M H_6 B_6 \\ \dot{H}_6 = +c_M L_6 x_6^+ - c_M H_6 B_6 - c_M x_6^- H_6 \\ \dot{B}_6 = +c_M L_6 x_6^+ - c_M H_6 B_6 \\ \dot{L}S_6 = -c_M L S_6 x_6^- + c_M H S_6 B S_6 \\ \dot{H}S_6 = +c_M L S_6 x_6^- - c_M H S_6 B S_6 \\ \dot{B}S_6 = +c_M L S_6 x_6^- - c_M H S_6 B S_6 \end{cases}$$

$$\bullet r^+ + r^- \xrightarrow{\eta} \emptyset \Rightarrow$$

$$\begin{cases} \dot{L}_r = -c_M r^+ L_r + c_M H_r B_r \\ \dot{H}_r = +c_M r^+ L_r - c_M H_r B_r - c_M r^- H_r \\ \dot{B}_r = +c_M r^+ L_r - c_M H_r B_r \\ \dot{L}S_r = -c_M r^- L S_r + c_M H S_r B S_r \\ \dot{H}S_r = +c_M r^- L S_r - c_M H S_r B S_r \\ \dot{B}S_r = +c_M r^- L S_r - c_M H S_r B S_r \end{cases}$$